

FOURTEENTH EUROPEAN ROTORCRAFT FORUM

Paper No. 53

**IDENTIFICATION OF XV-15 AEROELASTIC MODES
USING FREQUENCY-DOMAIN METHODS**

C. W. ACREE, JR.
NASA Ames Research Center
Moffett Field, California

MARK B. TISCHLER
Aeroflightdynamics Directorate,
U. S. Army Aviation Research and Technology Activity
Moffett Field, California

20-23 September, 1988
MILANO, ITALY

ASSOCIAZIONE INDUSTRIE AEROSPAZIALI
ASSOCIAZIONE ITALIANA DI AERONAUTICA ED ASTRONAUTICA

IDENTIFICATION OF XV-15 AEROELASTIC MODES USING FREQUENCY-DOMAIN METHODS

C. W. Acree, Jr.
NASA Ames Research Center
Moffett Field, California

Mark B. Tischler
Aeroflightdynamics Directorate,
U. S. Army Aviation Research and Technology Activity
Moffett Field, California

SUMMARY

The XV-15 Tilt-Rotor wing has six major aeroelastic modes that are close in frequency. To precisely excite individual modes during flight test, dual flaperon exciters with automatic frequency-sweep controls were installed. The resulting structural data were analyzed in the frequency domain (Fourier-transformed). Modal frequencies and damping were determined by performing curve fits to frequency-response magnitude and phase data. Results are given for the XV-15 with its original metal rotor blades. Frequency and damping values are also compared with new predictions by two different programs, CAMRAD and ASAP.

INTRODUCTION

Distinctive features of the XV-15 Tilt Rotor are the large wing-tip pylons which house the engines, transmissions and pivoting mechanisms for each rotor (Fig. 1). The concentrated masses at the wing tips keep the modal frequencies fairly low. Also, aeroelastic coupling between each rotor and pylon is destabilizing. Consequently, close attention must be paid to potential whirl-mode flutter during flight test. The highest speeds are obtained in the cruise mode, making it the critical operating mode for aeroelastic stability. The problem is not unique to the XV-15 research aircraft, but is fundamental to any tilt rotor aircraft of similar configuration, such as the XV-3, for which extensive studies were done (Refs. 1 and 2), and the upcoming V-22 Osprey (Ref. 3). Reference 4 gives a good summary of the development of whirl-mode flutter analyses applying to tilt rotors. The impact of aeroelastic stability requirements on tilt-rotor design is discussed in Reference 5.

A thorough re-evaluation of XV-15 aeroelastics with the existing metal rotor blades was conducted in preparation for flight tests of new composite blades (Ref. 6). A critical requirement was to validate the new modal identification techniques within the existing XV-15 flight envelope before flying the new Advanced Technology Blades (ATBs). Accordingly, all flight-test data discussed in the present report and in Reference 7 are for the metal blades.

The XV-15 wing modes were excited with flaperon frequency sweeps, and frequency spectra of the resulting time-history data were generated with chirp z-transforms. Modal frequencies and damping were determined by performing curve fits to frequency-response magnitude and phase data. The analysis programs have been used successfully on other flight

data, notably for XV-15 aircraft flight dynamics (Refs. 8 and 9). In addition to the flight-data analyses, two different theoretical analyses, CAMRAD and ASAP, were employed to predict the modes using mathematical models of the XV-15.

Early results of the frequency-domain analysis were reported in Reference 7, along with modal predictions. Both the flight-test data analysis and the predictive programs were subsequently revised, sometimes extensively. The updated results are given herein. More general overviews of XV-15 structural dynamics, including previous flight-test data, are given in References 10 and 11.

This report presents discussions of the XV-15 aeroelastic modes and the flight-test techniques used to excite them; the analytical procedures used to extract modal frequencies and damping from flight-test data; and plots of estimated frequency and damping versus airspeed, including comparisons with values predicted by both CAMRAD and ASAP.

FLIGHT-TEST METHODS

The intent of the flight tests was to validate the frequency-domain modal identification method and to map out the dominant aeroelastic modes (defined in Figs. 2 and 3). Safe and efficient flight testing first requires understanding of structural behavior based on analytical predictions. The following paragraphs give a brief overview of the aeroelastic modes of interest and the experimental methods used to identify them.

Predictions of damping versus airspeed made by CAMRAD (Ref. 12) are plotted for each mode in Figure 4. For certain combinations of altitude, rotor speed, and power, at least one mode—notably, symmetric chord—will encounter flutter (damping $\rightarrow 0$) at a sufficiently high airspeed. Also, the symmetric torsion mode lies within the design rotor-speed range. Consequently, the rotor speed with the metal blades is restricted in cruise to 8.6 Hz (86% of 601 rpm) instead of the design minimum of 7.6 Hz. Except for the symmetric beam mode, all modes lie within about 2 Hz of each other; two—the antisymmetric chord and antisymmetric torsion modes—are within 0.1 Hz at low airspeeds. The predicted instability and restricted rotor-speed range make precise identification of individual modes necessary, and the close placement in frequency makes such identification difficult.

In earlier flight tests, frequency and damping were identified by a variety of techniques, primarily exponential decays with Prony analysis, and (limited) turbulence excitation with RANDOMDEC and frequency-domain analyses. However, more recent tests (Ref. 8) showed that frequency-sweep excitation was the most promising approach, provided that both flaperons were driven to selectively excite the symmetric and antisymmetric modes. Compared to exponential decays and turbulence excitation, the frequency-sweep method is less sensitive to noise and requires less flight time, making it the method of choice. (Ref. 10 lists the pros and cons of the different flight-test techniques, and Ref. 13 discusses the errors of the associated analytical methods.)

High-frequency, limited-authority servo actuators in series with the flaperon control linkages excited the modes. Symmetric modes were excited by driving the left and right flaperons in phase; antisymmetric modes were excited by driving the flaperons in opposite phase. An amplitude of 100% equalled ± 5 degrees of flaperon motion.

An electronic controller automatically swept the flaperons from 1 to 10 Hz, using a logarithmically increasing sweep rate of approximately ten cycles per octave (the sweep rate was proportional to frequency). This was faster than the rate recommended in Reference 14, but still slow enough to clearly reveal each mode. Three such sweeps in succession were performed at each test condition.

The flight conditions tested are discussed later in this report, under Flight Test Results.

ANALYSIS METHODS

The overall concept of the modal identification method used in this study is to first estimate the (nonparametric) frequency response $H(f)$ between the aircraft excitation and structural response, and then to determine the (parametric) modal damping and frequency by second-order model fitting.

Figure 5 illustrates the excitation of the aircraft by measurable and unmeasurable inputs $x(t)$ and $m(t)$; the measured response $y(t)$ is corrupted by measurement noise $n(t)$. If the measurable and unmeasurable inputs and measurement noise are fully uncorrelated, then the unbiased (true average value) frequency response $H(f)$ may be estimated from the cross- and auto-spectral functions $G_{xy}(f)$ and $G_{xx}(f)$ as

$$\hat{H}(f) = \frac{G_{xy}(f)}{G_{xx}(f)} \quad (1)$$

(see Ref. 15 for a detailed discussion).

Figure 6 schematically shows the procedures used to conduct the analyses discussed herein. Each large block corresponds to a separate computer program. After each flight, the flaperon sweeps (input data) and the modal responses (output data) are loaded into the Tilt-Rotor Engineering Database System (TRENDS) for ease of subsequent access. Next, the Frequency Response Identification (FRESPID) program generates the spectral functions from the time histories in TRENDS. Finally, the modal parameters are determined by the curve-fitting program, NAVFIT. All computations are performed off-line (postflight).

TRENDS was developed by M. J. Bondi of NASA Ames Research Center and W. S. Bjorkman of Analytical Mechanics Associates, Inc. FRESPID was written by M. B. Tischler and J. G. M. Leung of Ames Research Center, and NAVFIT was originally developed by J. Hodgkinson and J. Buckley of McDonnell Douglas Aircraft (Ref. 16). For a detailed discussion of FRESPID and NAVFIT, see Reference 17.

The following sections briefly summarize the use of the programs with XV-15 aeroelastics data.

Fourier-Transform Computations

The first step is to Fourier-transform the flaperon excitation and structural response data using FRESPID. Flaperon motion is measured by LVDTs; wing responses are measured by separate beam, chord, and torsion strain gages near the wing roots (Fig. 2). Corresponding left and right transducers are summed or differenced, depending on the mode, to form composite inputs and outputs. If the two transducers are properly chosen, then the signals will be highly correlated and in phase for symmetric modes, and highly correlated but reversed in

phase for antisymmetric modes. Noise will not be correlated, thereby minimizing corruption of the spectral data.

Figure 7 shows the time histories of one flaperon sweep and the corresponding strain-gage response for the symmetric beam mode. Both signals are the sum of left and right transducer outputs; only symmetric content is visible. The decrease in flaperon amplitude with time, hence frequency, results from limited control-system frequency response. This effect is compensated for during the frequency-response calculations (Eq. 1).

FRESPID transforms the time-history data to the frequency domain by using a chirp z-transform, which improves on the conventional Cooley-Tukey Fast Fourier Transform (FFT) by allowing arbitrary resolution over a specified frequency range (Ref. 18). The dc components and linear drifts are first removed to prevent oscillation in the spectral calculations. Multiple runs are concatenated to form extended time-histories, which are digitally filtered and partitioned into several overlapping sections. Each section is scaled with a cosine weighting function ("Hanning window") to reduce side lobes and leakage (Ref. 19). The spectral content of each section is analyzed using the chirp z-transform. The total spectrum is finally determined by averaging the spectra of all of the sections.

Spectral Functions

Once the Fourier coefficients have been computed by the chirp z-transform, the auto- and cross-spectral functions, $G_{xx}(f)$, $G_{yy}(f)$, and $G_{xy}(f)$, are calculated by the formulas in Reference 15, then the frequency response, $H(f)$, by Equation 1. Figure 8 shows the magnitude and phase for the symmetric beam response to flaperon input, plotted in standard Bode form ($\text{dB} = 20 \log_{10} |H(f)|$). The magnitude plot clearly shows a second-order response peak, and the phase plot shows the 90-deg change in phase at the natural frequency.

The coherence function $\gamma^2(f)$ is also computed:

$$\gamma^2(f) = \frac{|G_{xy}(f)|^2}{G_{xx}(f) G_{yy}(f)} \quad (2)$$

For frequency responses, the coherence may be interpreted as that fraction of the output (response) spectrum that is linearly related to the input (excitation) spectrum (Ref. 19). If the system is perfectly linear and noise-free, the coherence will be unity. The coherence is a good measure of the quality of the data prior to application of the modal curve fit.

Figure 9 illustrates the coherence function corresponding to the frequency response shown in Figure 8. Reduced coherence above the natural frequency f_n was seen in all modes, especially near 1/rev (8.6 Hz at 86% rpm). Generally worse coherence was seen in the antisymmetric chord and symmetric torsion modes, falling off significantly at frequencies both above and below f_n . Even so, the coherence was always high enough near the peak response to allow good modal identification.

Frequency and Damping Calculations

Once frequency responses have been calculated by FRESPID, modal frequencies and damping are determined by curve-fitting the spectral data. Given a structure with natural frequency f_n and damping ratio ζ ($= 1/2$ structural damping coefficient g), the response can be well approximated by a quadratic second-order model of the form

$$H_m(f) = \frac{K}{1 - (f/f_n)^2 + i2\zeta f/f_n} \quad (3)$$

Only such models were used in the present study, as appropriate for structural analysis. (The gain K is determined largely by the sensitivities of the aircraft transducers, and has no direct bearing on aeroelastic stability. See Ref. 20 for an illustration of the potentially misleading effects of gain variations.)

The curve-fitting program NAVFIT is a general multimode, high-order analysis using both magnitude and phase data. The user specifies a frequency range to be fitted and initial estimates of f_n , ζ , and K . Phase shifts caused by unmodeled higher modes or 1/rev are fitted with a time delay. An iterative algorithm systematically varies f_n , ζ , and K to get the best fit, based on 50 frequency points.

The model is fitted by minimizing a cost function based on the squares of both magnitude and phase errors. The relative weights of the magnitude and phase errors are chosen to yield results equivalent to equal weighting of the real and imaginary parts of the complex frequency response (Ref. 17). To emphasize the most reliable data, there is a separate weighting of the errors by an exponential function of the coherence at each frequency point (Ref. 9). This is an improvement over the earlier use of a cosine weighting function for points near the peak (Ref. 7), because the coherence is a direct measurement of data quality.

An example of the use of NAVFIT to determine frequency and damping for the symmetric beam mode is given in Figure 8. Note that magnitude and phase are both fitted with a second-order frequency response.

The development of frequency-domain techniques for use with the XV-15 has been ongoing at NASA Ames Research Center for some time. Early results of their application to aeroelastics were reported in Reference 7, including an alternative method that used the cross-spectrum between the left and right transducer output data; that method proved useful for analyzing the chord modes. Since then, important improvements have been made to the flight-test data analyses, including refinements to the transducer signal processing and associated sum-and-difference procedures used on the time-history data. These improvements permitted frequency responses to be used exclusively for all modes. The values of the estimates given in the following sections of this report are slightly different from those of Reference 7 and reflect the improved data analyses, including coherence weighting procedures.

FLIGHT-TEST RESULTS

Figure 10 shows the portions of the XV-15 flight envelope covered during the aeroelastics flight tests. Because the aircraft had already been cleared to fly the envelope shown, the frequency sweeps were concentrated within a fairly narrow region so as to more rigorously verify the frequency-domain technique. The most complete data set was acquired at 3000-m density altitude at 86% rotor speed (8.6 Hz), with a typical gross weight near 6100 kg. The airspeed range was 330 km/hr true airspeed (180 knots), the normal speed for conversion to airplane mode, up to 490 km/hr (260 knots), the torque-limited maximum speed for level flight. Only these data are reported here. (Limited data were also taken at 1500 m and 4500 m at 86% rotor speed, and at 3000 m at 98% rotor speed.)

Ideally, several replications (i.e., several complete sets of sweeps) would have been performed at each flight condition. As this would have taken far too much flight-test time, an easily repeatable flight condition of 330 km/hr at 3000 m was chosen for multiple replications to explicitly test for scatter in the frequency and damping estimates. The XV-15 normally reaches this condition immediately after conversion to cruise mode, making it an efficient baseline point.

Earlier flight tests (Ref. 10) showed interaction of the Stability Control Augmentation System (SCAS) with modal responses, which was eliminated by modification of the SCAS. To ensure that there were no other interactions, each part of the automatic flight control system—the SCAS, the Attitude Retention System (ARS), and the Force Feel System (FFS)—was individually turned off during three series of sweeps at the baseline point. In a comparison of the results with the other baseline estimates, no statistically significant differences were noted. These data were subsequently included in the baseline data.

Figures 11-16 summarize the frequency and damping results for all six modes. All data are plotted against true airspeed, the critical value for aeroelastics. The frequency-domain method yields low scatter at the baseline point and good consistency between airspeeds. As demonstrated in Reference 7, these results represent a considerable improvement over the earlier exponential-decay method. (Individual modes are discussed in detail below.)

Numerical results of the frequency-domain method are summarized in Table 1 for the 330-km/hr baseline point. Listed for each mode are the averages of damping ($\bar{\zeta}$) and frequency (\bar{f}_n) and their respective standard deviations (σ_{ζ} and σ_{f_n}), which are measures of the scatter among the estimates. The standard deviations of the damping range from 7% to 9% of the average values, while the standard deviations of the frequency are all less than 1%.

In a few cases—notably, antisymmetric torsion—a statistically significant fraction of the scatter can be explained by weight changes caused by fuel burnoff. It is not practical to collect all flight data at exactly the same fuel state. Therefore, the values given in Table 1 represent realistically achievable performance of the frequency-sweep flight-test method.

Analytical Predictions

A detailed assessment of all available predictive methods is beyond the scope of this paper (see Ref. 4). Two different programs—ASAP and CAMRAD—were used in order to avoid biasing the comparisons with flight data toward one particular type of analysis. The ASAP and CAMRAD predictions are plotted with the frequency-domain estimates in Figures 11-16.

The ASAP predictions of frequency and damping were made by Bell Helicopter Textron; the CAMRAD predictions were made by NASA. ASAP is a new analysis proprietary to Bell; it is similar in concept to PASTA (Ref. 21), but completely rederived and reprogrammed. ASAP was originally developed for the V-22 program, and was modified by Bell for the XV-15 predictions given here. The CAMRAD model used here is based on that of Reference 5, but updated to have the correct precone for the steel hubs plus new NASTRAN mode shapes (necessitated by the heavier hubs). The ASAP and CAMRAD predictions were all based on nominal flight-test conditions of 3000 m altitude, 86% rotor speed and 5900 kg gross weight. (Reference 7 used predictions from DYN4, a less sophisticated program

replaced by ASAP, and from an older CAMRAD model that incorporated a less accurate representation of the XV-15.)

Both CAMRAD and ASAP rely on external sources of structural modes data for the wing. All predictions given here use natural frequencies, mode shapes and generalized masses generated by NASTRAN, with structural and aerodynamic damping values derived from a rotors-off wind tunnel test of an aeroelastic model of the V-22. No comparable data exist for the XV-15 itself that have been directly verified by a structural test. The values of zero-airspeed frequencies f_s and damping ζ_s used for all predictions reported herein are given in Figure 3. (Ref. 22 describes a method (also used in Refs. 5 and 7) of empirically adjusting CAMRAD damping estimates which forces a closer fit to the flight data. That method was not applied here in order to keep the CAMRAD and ASAP models similar.)

The present study was not designed to permit rigorous comparisons between ASAP and CAMRAD. However, the following observations can be made. ASAP and CAMRAD gave very similar predictions, usually matched more closely to each other than to the NAVFIT estimates. The differences between the ASAP and CAMRAD predictions in Figures 11-16, where both analytical programs used the same assumptions of zero-airspeed structural damping, were generally much less than the differences between the CAMRAD model used here and that of Reference 7, which used structural damping values derived by the method of Reference 22. These results imply that errors in the NASTRAN model of the XV-15 and uncertainties in the estimation of structural damping are at least as important as the differences between ASAP and CAMRAD (at least in their present versions). Accordingly, increased attention should be given to improving and verifying the NASTRAN model of the XV-15, including zero-airspeed structural damping.

Comparative Statistics

As shown in Figure 4, the slope of damping versus airspeed can become very steep as a mode approaches flutter. Consequently, accurate predictions and measurements of the trend of damping with airspeed are at least as important as those of overall magnitude. The key requirement is to detect a change in the trend of damping with airspeed as a stability boundary is approached. Most modes initially show increasing damping with airspeed, but change to a negative slope at a sufficiently high airspeed (Fig. 4).

In order to make statistical comparisons between the estimates and the predictions, the frequency and damping results were curve-fitted against airspeed over the range of speeds tested in flight. Linear fits were used, partly because almost all predictions show nearly constant slopes within the flight-test airspeed range, and partly because the NAVFIT standard errors will be conservative measures of scatter if the true variations are in fact nonlinear. The standard error is a measure of the scatter about a fitted curve (analogous to the standard deviation about a point). The curve fit results are summarized in Tables 2 and 3 for each mode.

Tables 2 and 3 denote whether the slopes of the NAVFIT estimates (derived from flight data) show statistically significant differences from the CAMRAD and ASAP predictions, based on a 5%-level t -test. The large number of significant variations from the predictions actually speaks well of the frequency-domain technique: had the scatter in any given NAVFIT estimate been very large, a t -test would not have shown a significant difference, even if the true slopes were unequal.

The statistical tests indicated in Tables 2 and 3 are potentially misleading because there are uncertainties in the curve fits to the predictions caused by numerical round-off errors and by the small number of data points. Furthermore, it is unlikely that the standard errors would be as low as those given in the tables if fully replicated flight data were available. Nevertheless, the tests are adequate to illustrate the main thrust of this effort: that the frequency-domain method is sufficiently sensitive and repeatable to reliably detect seriously erroneous predictions of aeroelastic stability, hence providing confidence in a safe envelope expansion. It is not valid to go beyond that and attempt to judge which predictive program is superior, especially in light of the unverified NASTRAN data.

Care should be taken when comparing other published data with the new frequency-sweep results. No complete set of exponential-decay data exists for an aircraft configuration that exactly matches that for the new data. Three different versions of rotor hubs have been flown: titanium hubs with either 2.5° or 1.5° precone, and steel hubs with 1.5° precone. The frequency-sweep results are for 1.5° steel hubs. Other reports on XV-15 aeroelastics (e.g., Refs. 10 and 11) sometimes include data for the aircraft operated by Bell, which is not identical to the aircraft operated by NASA, or for different hubs. These additional configurations are thought to have slightly different aeroelastic behavior.

Individual Modes

Symmetric beam (Fig. 11)—The CAMRAD and ASAP predictions of natural frequency f_n are about 0.1 Hz lower than the NAVFIT frequency-domain estimates derived from the flight data, and slowly decrease with airspeed, as do the estimates. The predicted values of damping ζ are slightly lower in magnitude and increase more slowly with airspeed than the flight-data estimates. The dip in the ASAP predictions of ζ at 325 km/hr also occurs in the CAMRAD predictions, but at a lower airspeed (visible for the sea level predictions in Fig. 4). The 280-km/hr point was not included in the ASAP curve fit (Table 3).

Antisymmetric beam (Fig. 12)—The predictions of f_n are about 0.5 Hz higher than the estimates, and decrease with airspeed unlike the slowly increasing estimates. The predictions of ζ average at least 0.02 (2% critical damping) below the estimates and increase with airspeed; the estimates are nearly constant (their slope is not significantly different from zero).

Symmetric chord (Fig. 13)—The predictions of f_n are about 0.2 Hz below the estimates, and decrease with airspeed at roughly the same rate. The predictions of ζ are as much as 0.02 lower than estimated and increase less rapidly with airspeed, more noticeably for CAMRAD.

Antisymmetric chord (Fig. 14)—The predictions of f_n are slightly greater than estimated, and do not follow the slope of the estimates. The predictions of ζ are up to 0.02 greater than estimated, with positive slopes (especially ASAP). The apparent dip in the estimated damping at 420 km/hr is thought to be caused by scatter.

Symmetric torsion (Fig. 15)—The predictions of f_n lie within 0.1 Hz of the estimates. It cannot be determined whether the change in the slope of the estimates above 420 km/hr is an accurate reflection of XV-15 aeroelastic behavior, or is an illusion caused by scatter. The predictions of ζ are more than 0.01 lower than estimated, and show significantly slower rise with airspeed.

Antisymmetric torsion (Fig. 16)—The predictions of f_n are generally over 1 Hz greater than the estimates, and decrease more slowly with airspeed. The predictions of ζ are 0.04 to 0.06 lower than estimated, and increase much less rapidly with airspeed. There is an abrupt decrease at the last, highest-speed estimate of ζ , but it cannot be determined whether this reflects a true change in slope or whether it is merely caused by scatter.

Although antisymmetric chord and torsion, as estimated by NAVFIT, have the same natural frequency at the baseline point (Table 1), there is a statistically significant difference between the estimated slopes of the two modal frequencies (Table 2). Furthermore, the damping values for these two modes are clearly different in magnitude and slope (Figs. 14 and 16). This shows that the chord and torsion strain gages have low enough crosstalk for the frequency-domain method to resolve two very close modes.

In a few cases, the frequency-domain estimates appear to vary nonlinearly with airspeed, contrary to the roughly linear predictions, but it has not been proven that any such instance indicates a real aeroelastic phenomena. Even at the worst, the overall consistency of the estimates is adequate for reliable detection of incipient aeroelastic instability, which is the goal of this development effort.

CONCLUSIONS AND RECOMMENDATIONS

Frequency-sweep excitation combined with frequency-domain analysis was demonstrated to be a reliable and efficient way of determining XV-15 aeroelastic behavior from flight data, permitting good estimations of all modes. Dual-flaperon excitation plus sum-and-difference signal processing yielded good time-history data for each mode, and chirp z-transform Fourier analysis generated excellent spectra. Based on curve fits to frequency responses, the estimates of modal frequencies and damping varied linearly with airspeed and were highly repeatable at a reference flight condition (within less than 1% relative error for natural frequency and 9% relative error for damping). Because of the good analytical results shown here, and the reduced flight-test time compared to other methods, the frequency-sweep method has been chosen to support flight tests of the new XV-15 composite blades (ATBs), now underway.

Obvious improvements are to replicate all flight-test conditions beyond the baseline point and to extend the speed range to both higher and lower airspeeds, thereby permitting more accurate determination of the trends of frequency and damping with airspeed, with more complete statistics. Gross weight cannot be kept constant, but by deliberately introducing a greater range of weights among the test conditions, the effects of weight could be more reliably determined and distinguished from the effects of airspeed (given enough replications).

A more subtle change is to reduce the speed at which the flaperons sweep through the frequency range. The ideal procedure is to have very slow sweeps, repeated many times at each test condition, with several replications of each condition. Unfortunately, this would require an excessive amount of flight-test time. Initial tests of the ATBs are planned to use slower sweeps over a reduced frequency range and to explicitly study the trade-off in accuracy between sweep rate and number of sweeps per test point.

Improvements are also possible for the analytical predictions. CAMRAD and ASAP are both being continually upgraded, and new predictions will be made for the XV-15 as improved programs become available. A ground vibration test of the XV-15 using the frequency-sweep techniques described here is planned, with the goal of obtaining better estimates of zero-airspeed structural frequencies and damping. Such results could be fed into the CAMRAD and ASAP models for further improvements in the predictions of aeroelastic stability.

ACKNOWLEDGEMENTS

The authors wish to thank J. R. Gillman of the Boeing Helicopter Corporation for providing upgrades to the CAMRAD model of the XV-15, and S. K. Yin of Bell Helicopter Textron for the ASAP predictions.

REFERENCES

- 1) Hall, W. E. *Prop-Rotor Stability at High Advance Ratios*. Journal of the American Helicopter Society, vol. 11, no. 2, pp. 11-26, April 1966.
- 2) Edenborough, H. K. *Investigation of Tilt Rotor VTOL Aircraft Rotor-Pylon Stability*. AIAA Paper no. 67-17, presented at the 5th Aerospace Sciences Meeting, New York, N.Y., Jan. 23-26, 1967; and Journal of Aircraft 5(6), March-April 1968.
- 3) Popelka, D.; Sheffler, M.; and Bilger, J. *Correlation of Test and Analysis for the 1/5-Scale V-22 Aeroelastic Model*. Journal of the American Helicopter Society, vol. 32, no. 2, pp. 21-33, April 1987.
- 4) Ormiston, R. A.; Warmbrodt, W. G.; Hodges, D. H.; and Peters, D. A. *Rotorcraft Aeroelastic Stability*. Presented at the NASA/Army Rotorcraft Technology Conference, NASA Ames Research Center, California, March 17-19, 1987. Also NASA CP-2495, 1988, vol. 1, pp. 353-529.
- 5) Johnson, W.; Lau, B. H.; and Bowles, J. V. *Calculated Performance, Stability, and Maneuverability of High-Speed Tilting-Prop-Rotor Aircraft*. NASA TM-88349, Sept. 1986.
- 6) Alexander, H. R.; Maisel, M. D.; and Giulianetti, D. J. *The Development of Advanced Technology Blades for Tiltrotor Aircraft*. Presented at the 11th European Rotorcraft Forum, London, England, Sept. 10-13, 1985.
- 7) Acree, C. W. and Tischler, M. B. *Using Frequency-Domain Methods to Identify XV-15 Aeroelastic Modes*. Presented at the SAE International Powered Lift Conference, Santa Clara, California, December 7-10, 1987. Also NASA TM 100033, November 1987; and USAAVSCOM TR-87-A-17.
- 8) Tischler, M. B.; Leung, J. G. M.; and Dugan, D. C. *Frequency-Domain Identification of XV-15 Tilt-Rotor Aircraft Dynamics*. Presented at the 2nd AIAA/AHS/IES/SETP/SFTE/DGLR Flight Testing Conference, Las Vegas, Nevada, Nov. 16-18, 1983.
- 9) Tischler, M. B. *Advancements in Frequency-Domain Methods for Rotorcraft System Identification*. Presented at the Second International Conference on Basic Rotorcraft Research, College Park, Maryland, February 1988.
- 10) Schroers, L. G. *Dynamic Structural Aeroelastic Stability Testing of the XV-15 Tilt Rotor Research Aircraft*. NASA TM-84293, Dec. 1982
- 11) Bilger, J. M.; Marr, R. L.; and Zahedi, A. *In-Flight Structural Dynamic Characteristics of the XV-15 Tilt Rotor Research Aircraft*. AIAA-81-0612.
- 12) Johnson, W. *A Comprehensive Analytical Model of Rotorcraft Aerodynamics and Dynamics. Part I: Analysis Development*. NASA TM 81184, June 1980; and USAAVSCOM TR-80-A-7.

- 13) Johnson, W. *A Discussion of Dynamic Stability Measurement Techniques*. NASA TM X-73,081, November 1975.
- 14) Flannelly, W. G.; Fabunmi, J. A.; and Nagy, E. J. *Analytical Testing*. NASA CR-3429, May 1981.
- 15) Bendat, J. S. and Piersol, A. G. *Engineering Applications of Correlation and Spectral Analysis*. John Wiley and Sons, Inc., New York, 1980.
- 16) Hodgkinson, J. and Buckley, J. *NAVFIT General Purpose Frequency Response Curve Fit (Arbitrary Order)*. McDonnell Aircraft Company, St. Louis, Mo., Oct. 1978.
- 17) Tischler, M. B. *Frequency-Response Identification of XV-15 Tilt-Rotor Aircraft Dynamics*. NASA TM 89428, May 1987; and USAAVSCOM TM-87-A-2.
- 18) Rabiner, L. R. and Gold, B. *Theory and Application of Digital Signal Processing*. Prentice-Hall, Inc., Englewood Cliffs, New Jersey, 1975.
- 19) Otnes, R. K. and Enochson, L. *Applied Time Series Analysis*. John Wiley and Sons, Inc., New York, 1978.
- 20) Houbolt, J. C. *On Identifying Frequencies and Damping in Subcritical Flutter Testing*. Flutter Testing Techniques, NASA SP-415, 1976, pp. 1-41.
- 21) Kvaternick, R. G. *Studies in Tilt-Rotor VTOL Aircraft Aeroelasticity*. Ph.D. Thesis, Case Western Reserve University, Cleveland, Ohio, June 1973
- 22) Johnson, W. *An Assessment of the Capability To Calculate Tilting Prop-Rotor Aircraft Performance, Loads, and Stability*. NASA TP-2291, March 1984.

Table 1. XV-15 wing modes at the baseline flight condition
(statistics are based on 8 data points)

Mode	$\bar{\zeta}$ % critical damping	σ_{ζ} % critical damping	σ_{ζ} % relative error	\bar{f}_n Hz	σ_{f_n} Hz	σ_{f_n} % relative error
Symmetric Beam	2.54	0.235	9.3	3.30	0.0084	0.25
Antisymmetric Beam	6.09	0.398	6.5	5.90	0.0424	0.72
Symmetric Chord	3.94	0.326	8.3	6.33	0.0110	0.17
Antisymmetric Chord	3.89	0.349	9.0	7.25	0.0278	0.38
Symmetric Torsion	3.97	0.362	9.1	8.08	0.0205	0.25
Antisymmetric Torsion	6.07	0.406	6.7	7.25	0.0396	0.55

Table 2. Statistics for frequency versus airspeed

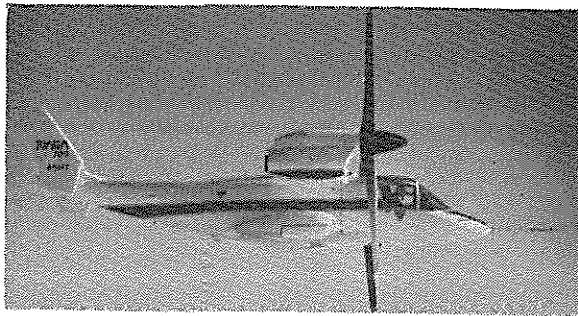
Mode	Frequency-Domain Estimates			Analytical Predictions	
	Standard error, Hz	Intercept, Hz	Slope, Hz / knot $\times 10^{-3}$	CAMRAD Slope, Hz / knot $\times 10^{-3}$	ASAP Slope, Hz / knot $\times 10^{-3}$
Symmetric Beam	0.00965	3.35	-0.265	-0.208	-0.296
Antisymmetric Beam	0.0350	5.67	0.127	-1.18*	-0.571*
Symmetric Chord	0.0159	6.54	-1.18	-1.30	-1.75*
Antisymmetric Chord	0.0296	7.08	0.893	-1.71*	-2.17*
Symmetric Torsion	0.0324	8.20	-0.684	-2.37*	-2.79*
Antisymmetric Torsion	0.0397	7.96	-3.98	-0.860*	-1.30*

* statistically significant difference between estimated and predicted slopes

Table 3. Statistics for damping versus airspeed

Mode	Frequency-Domain Estimates			Analytical Predictions	
	Standard error, % critical damping	Intercept, % critical damping	Slope, % critical damping per knot $\times 10^{-3}$	CAMRAD Slope, % critical damping per knot $\times 10^{-3}$	ASAP Slope, % critical damping per knot $\times 10^{-3}$
Symmetric Beam	0.197	1.13	7.86	2.88*	4.71
Antisymmetric Beam	0.358	6.59	-2.98	5.68*	5.69*
Symmetric Chord	0.307	2.14	10.2	1.08*	3.70
Antisymmetric Chord	0.373	4.53	-3.85	3.72	8.13*
Symmetric Torsion	0.376	-1.41	30.1	7.72*	10.11*
Antisymmetric Torsion	0.395	0.615	30.8	1.80*	3.33*

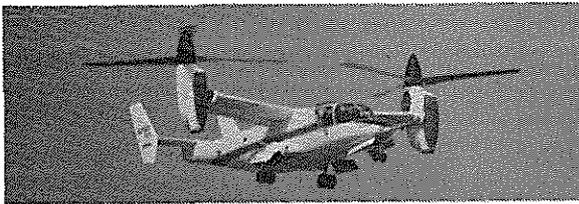
* statistically significant difference between estimated and predicted slopes



"CRUISE" FLIGHT MODE



"TILT-ROTOR" FLIGHT MODE



"HELICOPTER" FLIGHT MODE

Figure 1. XV-15 tilt-rotor research aircraft

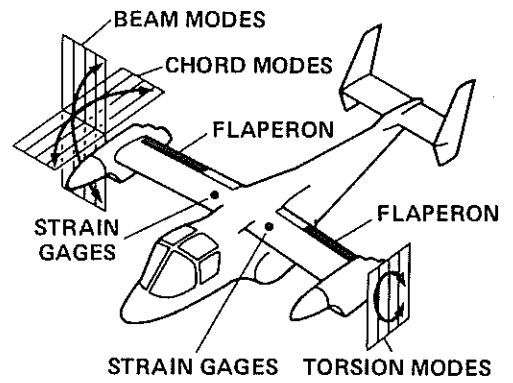


Figure 2. XV-15 aircraft, showing flaperons, strain gage locations, and wing modes

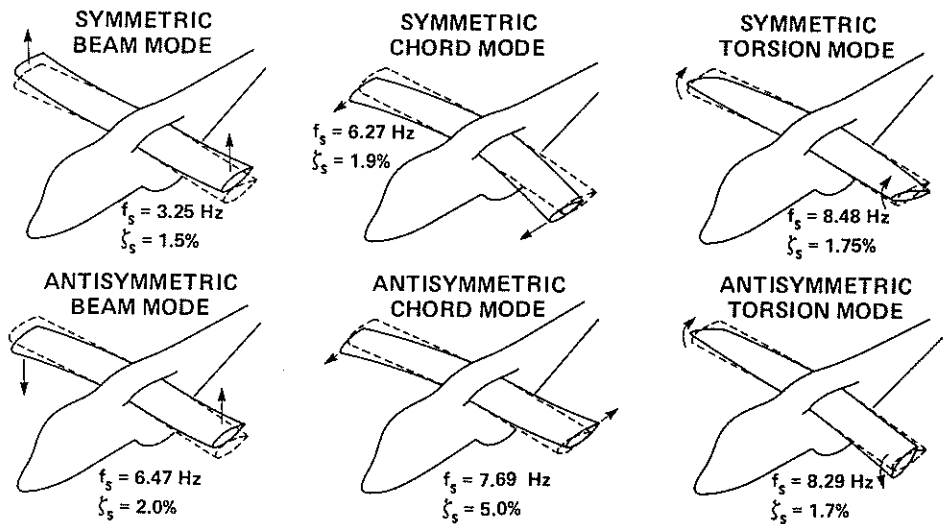


Figure 3. XV-15 wing modes, with zero-airspeed structural frequencies and damping

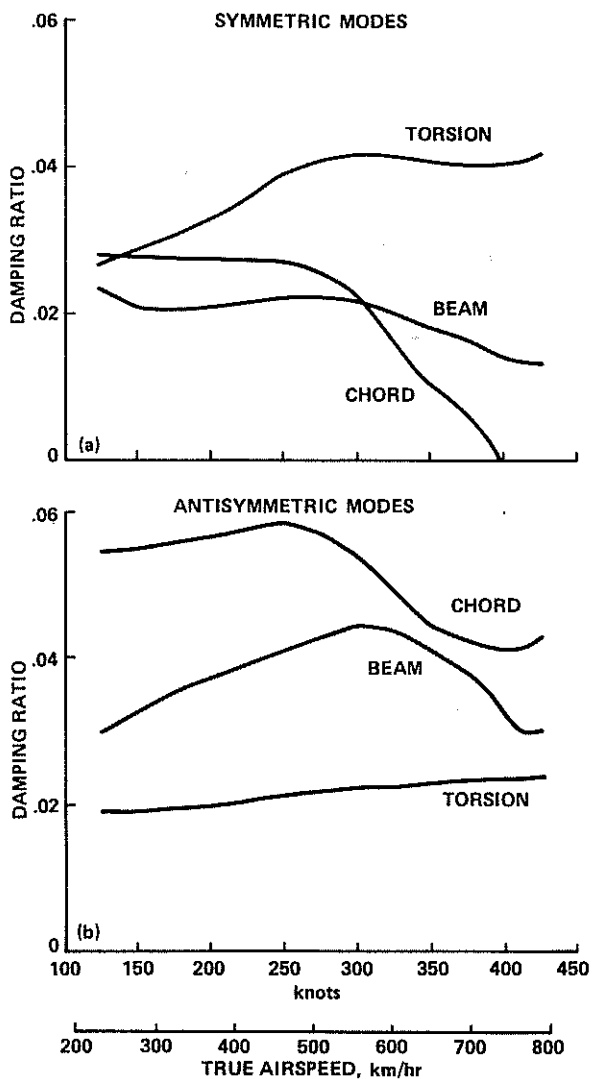


Figure 4. CAMRAD damping predictions for sea level, 86% rpm, and maximum $C_p/\sigma = 0.046$

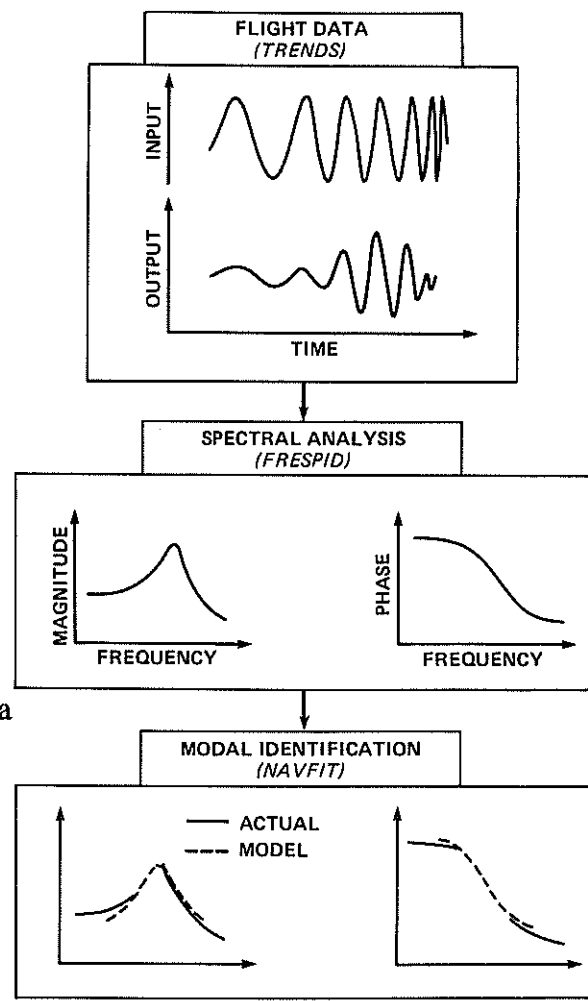


Figure 6. Data processing for frequency-domain modal identification

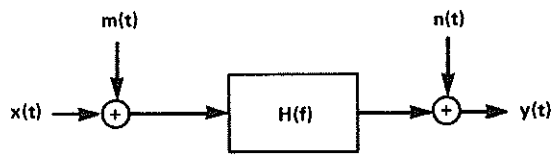


Figure 5. Signals and noise affecting frequency-response calculations

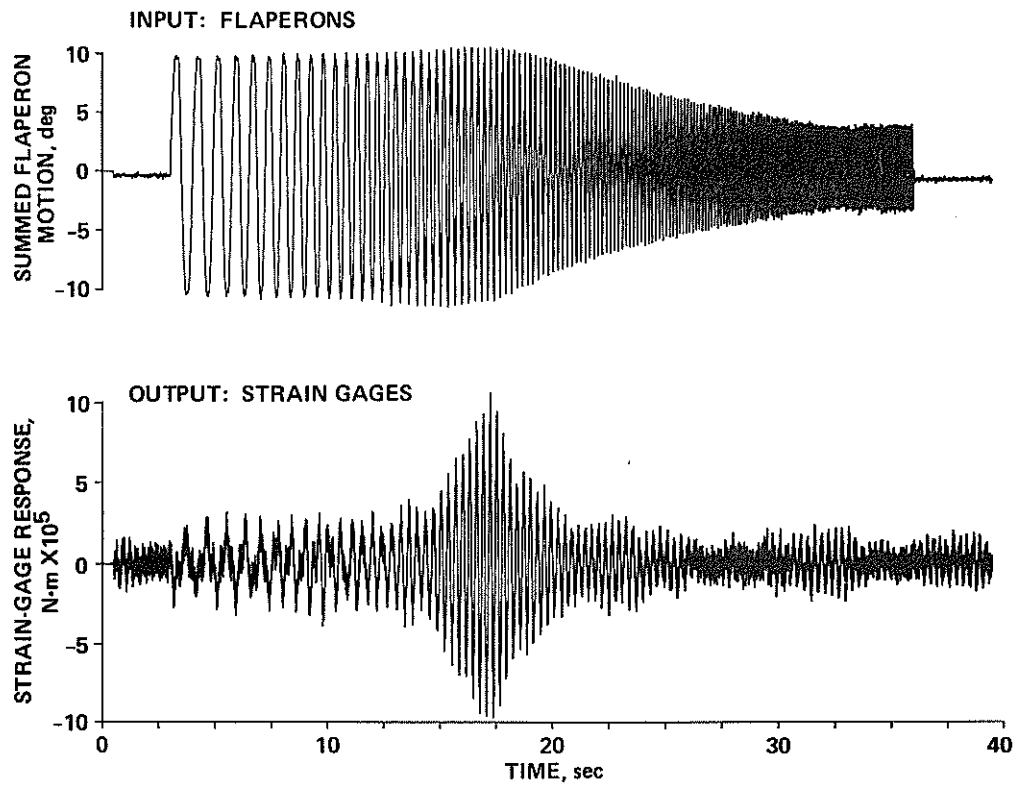


Figure 7. Input and output time-histories for one symmetric flaperon sweep (beam mode)

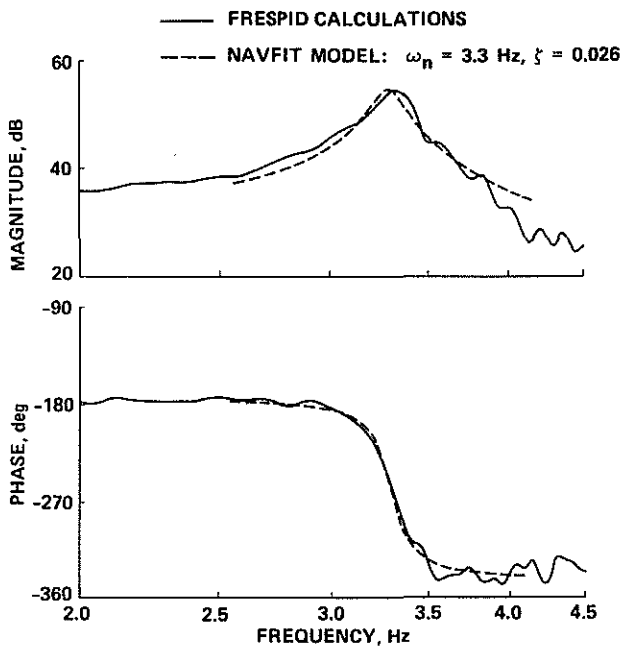


Figure 8. Symmetric beam mode frequency response

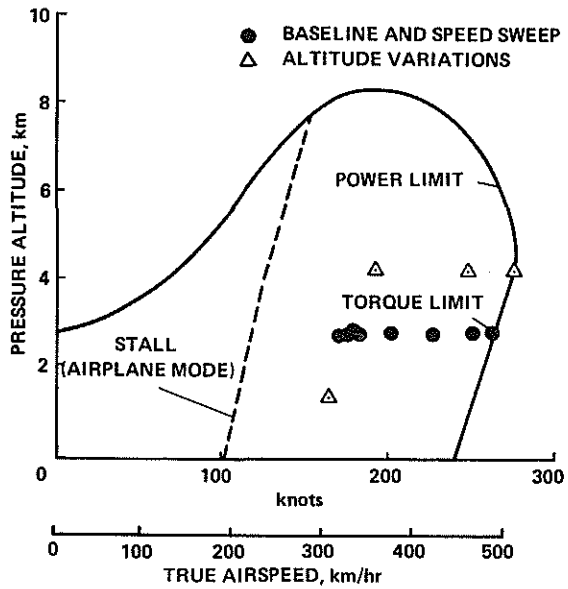


Figure 10. XV-15 level flight envelope, showing frequency-sweep test points

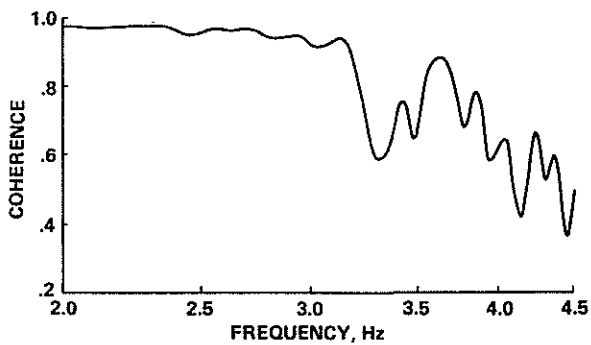


Figure 9. Coherence function $\gamma^2(f)$ for the symmetric beam mode

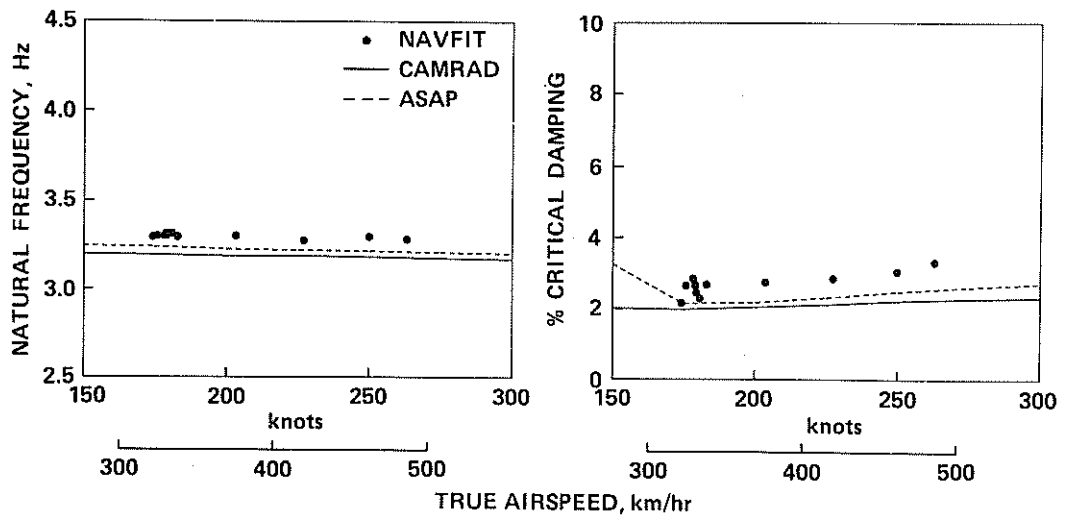


Figure 11. Flight-data estimates and analytical predictions of f_n and ζ for the symmetric beam mode

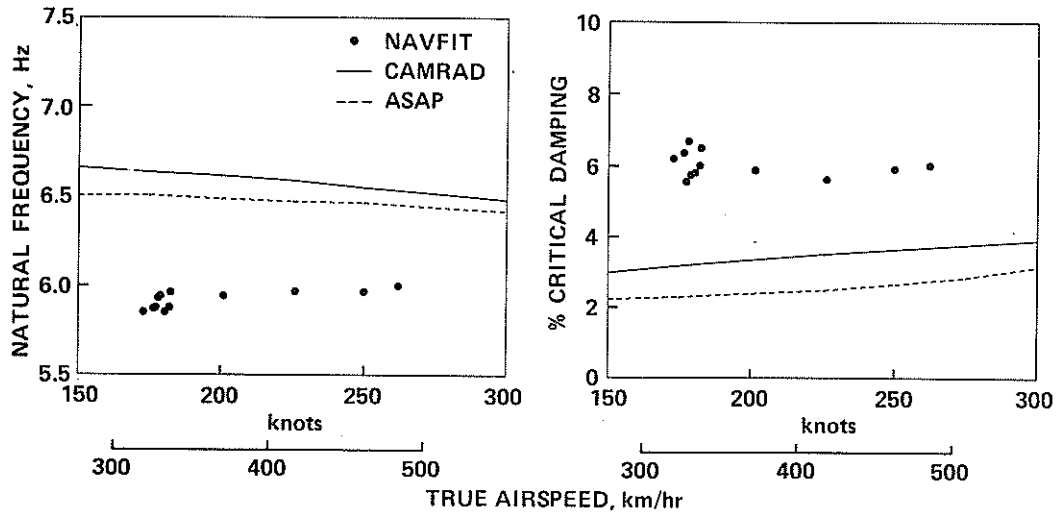


Figure 12. Flight-data estimates and analytical predictions of f_n and ζ for the antisymmetric beam mode

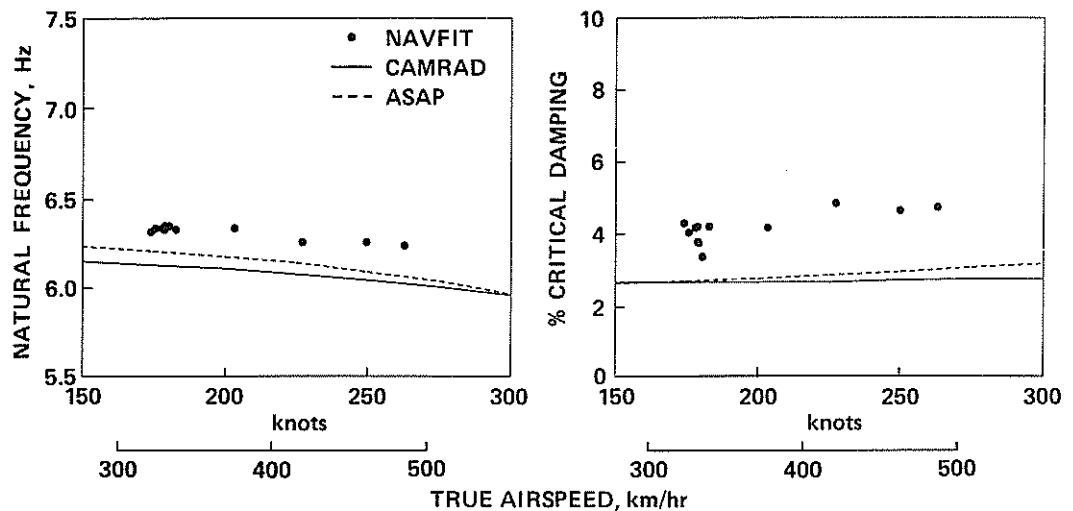


Figure 13. Flight-data estimates and analytical predictions of f_n and ζ for the symmetric chord mode

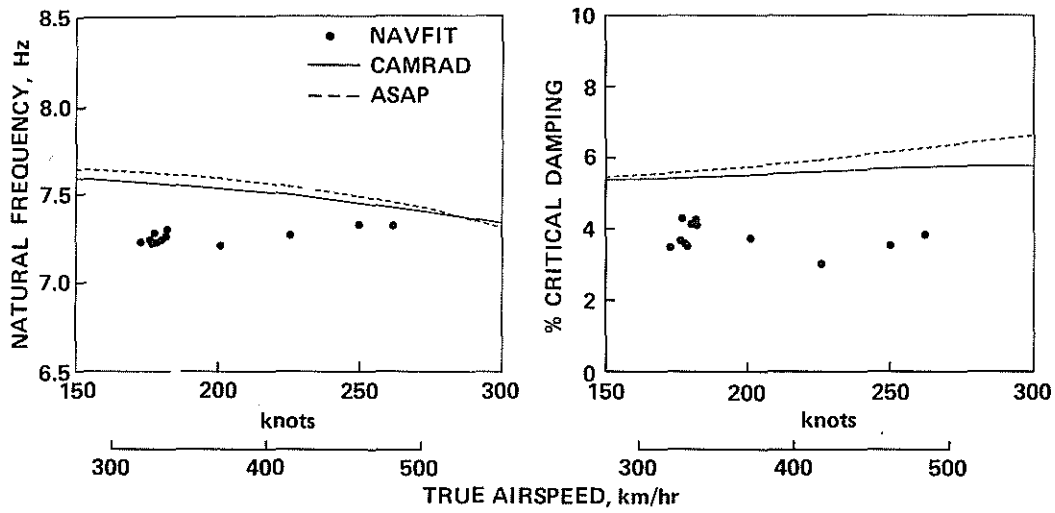


Figure 14. Flight-data estimates and analytical predictions of f_n and ζ for the antisymmetric chord mode

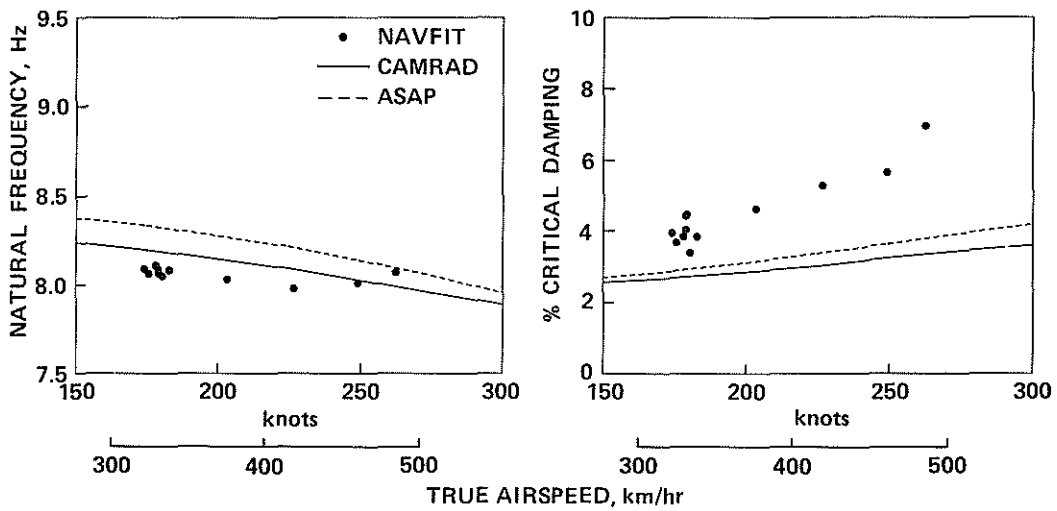


Figure 15. Flight-data estimates and analytical predictions of f_n and ζ for the symmetric torsion mode

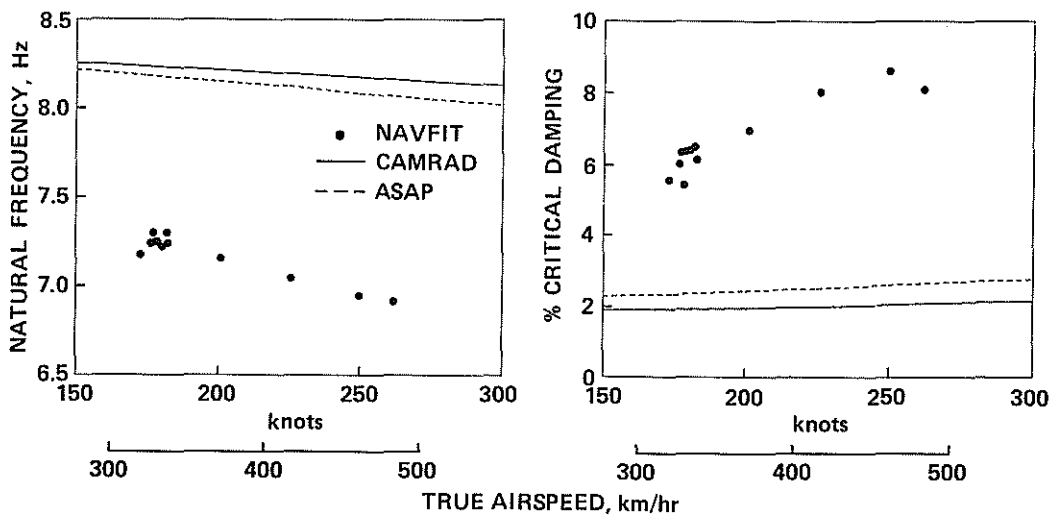


Figure 16. Flight-data estimates and analytical predictions of f_n and ζ for the antisymmetric torsion mode